Title	Design, simulation and characterization of wheatstone bridge structured metal thin film uncooled microbolometer
Author(s)	Ang, Wan Chia; Kropelnicki, Piotr; Tsai, Julius Ming Lin; Leong, Kam Chew; Tan, Chuan Seng
Citation	Ang, W. C., Kropelnicki, P., Tsai, J. M. L., Leong, K. C., & Tan, C. S. (2014). Design, simulation and characterization of wheatstone bridge structured metal thin film uncooled microbolometer. Procedia engineering, 94, 6-13.
Date	2014
URL	http://hdl.handle.net/10220/25084
Rights	© 2014 Chuan Seng Tan. Published by Elsevier Ltd. This is an open access article under the CC BY-NC-ND license (http://creativecommons.org/licenses/by-nc-nd/3.0/).

Available online at www.sciencedirect.com

ScienceDirect

Procedia Engineering 94 (2014) 6 – 13

Procedia Engineering

www.elsevier.com/locate/procedia

MRS Singapore - ICMAT Symposia Proceedings

7th International Conference on Materials for Advanced Technologies

Design, Simulation and Characterization of Wheatstone Bridge Structured Metal Thin Film Uncooled Microbolometer

Wan Chia Ang[a,b], Piotr Kropelnicki[a], Julius Ming Lin Tsai[a], Kam Chew Leong[c], Chuan Seng Tan[b,*]

[a]*Institute of Microelectronics, A*STAR (Agency for Science, Technology and Research), 11 Science Park Road, Science Park II, Singapore 117685*

[b]*School of Electrical & Electronics Engineering, Nanyang Technological University, 50 Nanyang Avenue, Singapore 639798*

[c]*GLOBALFOUNDRIES Singapore Pte Ltd, 60 Woodlands Industrial Park D, Street 2, Singapore 738406*

Abstract

It is demonstrated for the first time that the Wheatstone bridge structured metal thin film resistive uncooled microbolometer (in short, WB-bolometer) provides promising temperature sensitivity. This paper describes the design, simulation, and characterization of WB-bolometer using titanium nitride (TiN) thin film as the infrared (IR) sensing material. TiN thin film is designed into four resistors which are connected to each other in Wheatstone bridge configuration. The resistance value of each resistor changes with different rates upon IR absorption, which can be attributed to the difference in their associated thermal conductance. As a result, the bridge output voltage varies in response to the absorbed IR power. Simulation was employed to compare and characterize different designs of WB-bolometer. It was found that design with two sensing elements has the optimum performance. The proposed WB-bolometer is also capable of operating at elevated temperatures (> 250 °C) due to its adjustable and small initial offset voltage with minimum associated noise.

Selection and/or peer-review under responsibility of the scientific committee of Symposium [Symposium E - Solid-state devices for light emission and detection] – ICMAT

Keywords: Wheatstone bridge; uncooled microbolometer; metal thin film.

* Corresponding author. Tel.: +6567905636.
E-mail address: TANCS@ntu.edu.sg

Selection and/or peer-review under responsibility of the scientific committee of Symposium [Symposium E - Solid-state devices for light emission and detection] – ICMAT
doi:10.1016/j.proeng.2013.10.013

1. Introduction

IR radiation has many exciting and useful applications in different fields such as astronomy, military and surveillance [1]. Generally, there are two kinds of sensors for IR detection: photon detectors (cooled bolometer) and thermal detectors (uncooled bolometer) [2, 3]. Photon detectors convert the incoming IR photons into photocurrents that to be detected. Thermal detectors absorb the incoming IR radiation energy and convert it into heat energy, resulting in a temperature rise within the sensing material, which then changes certain material properties that are measurable. Compared with photon detectors, thermal detectors have a slower response time and weaker overall performance, but are more reliable and available at a much lower cost [4]. With the advancements in silicon micromachining technologies, micro-electro-mechanical-systems (MEMS) based thermal detectors have gained greater attention due to their advantages of ambient temperature operation, low weight, low power consumption, low cost, long term operation, and wide spectral response over photon detectors [4], which are advantageous to miniaturized and portable applications including firefighting, industrial inspections, energy conservation, medical monitoring, gas detection system, and automotive night vision [5].

Among different types of thermal detectors, semiconductor-based resistive uncooled microbolometers meet with most success because they are relatively easy to fabricate compared with pyroelectric bolometers [6-8] and have a better responsivity than thermoelectric bolometer [9-11]. However, they are tardily facing bottleneck in performance optimization. In addition to background and thermal fluctuation noise, they are susceptible to flicker and Johnson noise which inhibits their further improvement in sensitivity. On the other hand, the operating temperature is limited to 85 °C due to the decrease in sensing resistance and increase in system series resistance, resulting in an unacceptable low signal-to-noise ratio (SNR). The situation is even worse with self-heating effect, and this makes the readout a great challenge.

Metal thin films are well known wideband IR absorbers with very small heat capacity [12], which enable fast response with small thermal conductance design. In comparison with semiconductors IR absorbers, metal thin films have insignificant flicker noise. With the development of spectrometer applications, metal thin film microbolometers with a broadband sensitivity and fast response will be favorable. For conventional metal thin film microbolometers, the change of the voltage difference across the sensing material is being detected upon IR irradiation by an external readout circuit, typically a Wheatstone bridge and a differential amplifier [13].

This paper proposes a Wheatstone bridge structured metal thin film uncooled microbolometer at the device level. Having the IR detector constructed in WB-configuration, long interconnect loading as well as interface and noise pickup can be avoided [14]. For a perfectly balanced WB, power supply noise can be fully suppressed. Hence, the differential output voltage of the bridge may be amplified without degradation of the SNR. The resolution of the sensing system is only limited by the detector intrinsic noise, which is the Johnson noise. It is worth noting that WB-bolometer is capable of high temperature operations with high temperature stable metal thin films, attributed to the small overall system noise. With small and tunable differential output voltage, WB-bolometers have a huge advantage when they are built in large two-dimension array (focal plane array, FPA) to give an extremely fast readout. TiN is used as the IR-absorbing material due to their full compatibility with CMOS process and high temperature stability (up to 250 ^{o}C). Different designs of TiN WB-bolometer were characterized for their electro-thermal properties. For the design with the best performance in electro-thermal behaviors, the responsivity to IR absorption was also investigated.

2. Concept of Wheatstone bridge structured uncooled microbolometer

Wheatstone bridge is an electrical circuit consisting of four resistors, which constructed in the configuration as shown in Fig 1. It is normally used to measure the electrical resistance of the one having a non-constant or

unknown value by balancing and setting null the bridge output voltage, V_o. Eq. (1) relates V_o with the resistance ratio of both resistor branches and the supply voltage, V_s.

$$V_o = |V_a - V_b| = V_s \cdot \left| \frac{R3}{R1+R3} - \frac{R4}{R2+R4} \right| \tag{1}$$

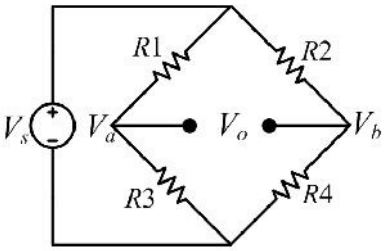

Fig. 1. Electrical circuit schematic of a Wheatstone bridge.

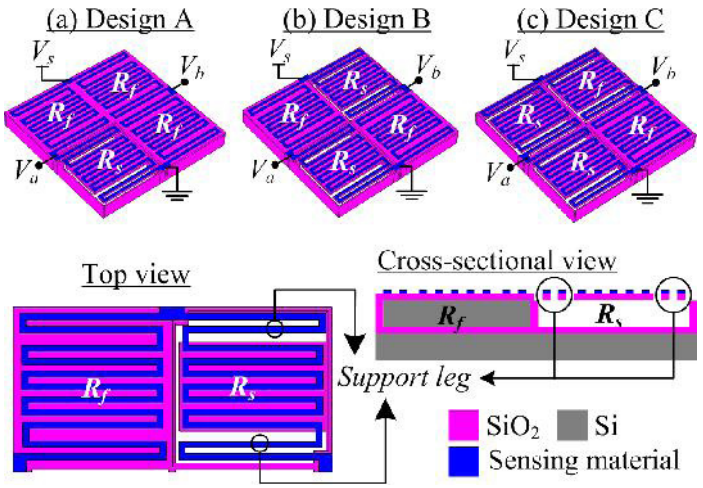

Fig. 2. Three possible designs of Wheatstone bridge microbolometer with (a) single, (b) double and (c) triple sensing elements.

For the purpose of IR sensing, Wheatstone bridge is utilized to detect the resistance change of the sensing material. The metallic sensing material is structured into four meander-like resistors with 0.5 μm line width, which are connected to each other and make up a 25 × 25 μm^2 pixel size. Each resistor plays a role as either sensing element (R_s) or reference element (R_f). In this work, three designs (see Fig 2) with different combination of R_s and R_f are compared. R_s is built on a 100 nm freestanding silicon dioxide (SiO_2) membrane with long thermal isolation legs while R_f is directly constructed on silicon (Si) substrate with 100 nm SiO_2 electrical isolation layer to have good heat dissipation path. Both R_s and R_f will be exposing to IR. Upon IR irradiation, the R_s resistance will change due to temperature rise while R_f resistance will remain almost constant. The difference in resistance changes of R_s and R_f disrupts the balance of the two resistor branches of the Wheatstone bridge, thereby giving rise to the change of V_o. The resistance change of R_s can be predicted by Eq. (2).

$$R_s(T) = R_s(0) \cdot [1 + \alpha \cdot \Delta T] \tag{2}$$

where $R_s(T)$ is the R_s resistance at temperature of T, R_s (0) is the R_s resistance at 0 °C, α is the linear temperature coefficient of resistance (TCR) and ΔT is the temperature rise due to IR absorption.

3. Thermal characterization of TiN

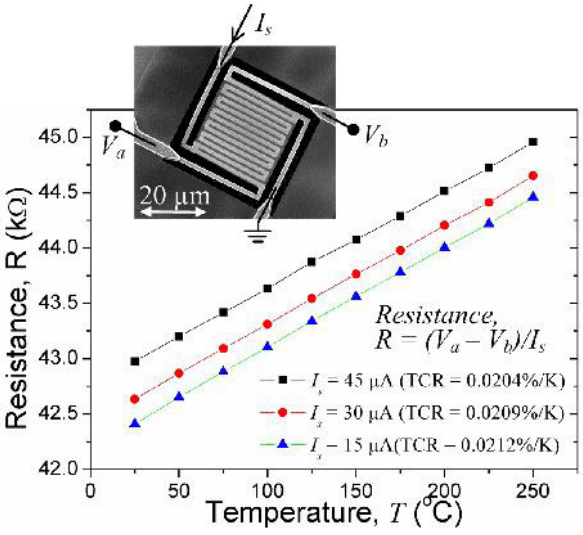

Fig. 3. Resistance variation of TiN Kelvin test structure with temperature.

In this work, a 15 nm thick TiN thin film was used as the IR sensing element. In order to give more accurate simulation results, the TiN thin film TCR was first obtained. A Kelvin test structure was fabricated on the 100 nm thick freestanding SiO_2 membrane as depicted in the inset of Fig 3. The Kelvin test structure has the TiN resistor line width of 1.0 μm and support leg width of 1.5 μm. It was clamped on the temperature chuck and was heated slowly in a vacuum chamber to achieve thermal equilibrium. Its resistance was obtained by four-point resistance measurement with different values of constant current supply, I_s. The resistance variation with temperature is plotted in Fig 3. The average TCR of a 15 nm TiN thin film was found to be about 0.020 %/K, which agrees well with the reported value [15, 16]. With increasing I_s, the TCR value of TiN thin film resistor is degraded due to the increasing Joule heating effect.

4. Design and simulation analysis

4.1. Electro-thermal behavior

COMSOL Multiphysics simulation tool was first employed to predict the response of the three WB-bolometer designs to the Joule heating effect. The temperature dependent electrical conductivity of TiN was obtained from Section 3. The rest of the material properties of SiO_2 and TiN used in this steady-state simulation are inputted from the database of Material Library of COMSOL Multiphysics as listed in Table 1.

Heat loss is mainly through conduction from SiO_2 membrane to the Si substrate. Convection loss could be ignored as the WB-bolometer was operated under vacuum condition. Radiation loss is also negligible because of its relatively small effect at temperature up to 573 K. The whole device was defined to have perfect thermal isolation and operate at an initial temperature of 293.15 K. All the electrical boundaries of the device were set to electrical isolation except those for electrical potential and ground defined boundaries. Heat source is generated from the Joule heating effect of the TiN resistors.

Table 1. Material properties of SiO_2 and TiN used in electro-thermal simulation

Material	SiO_2	TiN
Thermal conductivity [W/(m·K)]	-0.99+1.82e-2*T-5.29e-5*T^2+7.55e-8*T^3	3.40+1.32e-3*T
Density [kg/m^3]	2200	5220
Heat capacity [J/(kg·K)]	61.5+1.93*T+4.46e-3*T^2-1.70e-5*T^3	-2.0e7*T^{-2}+805.5+6.36e-2*T
Electrical conductivity [S/m]	-	1/(2.25e-6*(1+2e-4*(T-293.15)))

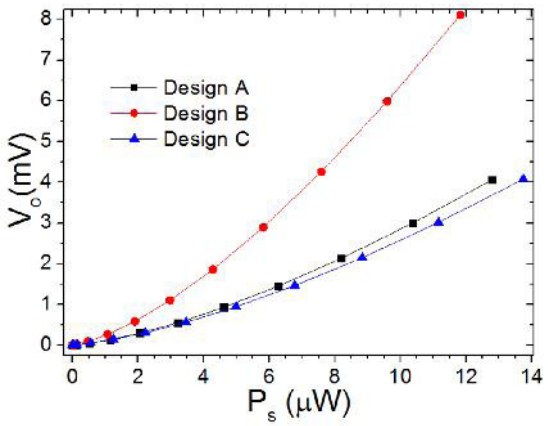

Fig. 4. Simulated V_o of the three WB-bolometer designs at different P_s levels.

Fig 4 shows the V_o variation of the three WB-bolometer designs at different power supplies, P_s. Design B has a responsivity at least twice compared with that of another two designs at all P_s levels. This is because the two R_s are located opposite to each other, giving rise to an opposing change in V_a and V_b, thus the highest V_o responsivity to Joule heating.

4.2. Temperature profile and thermal response

The figure-of-merit (FOM) of an IR detector is governed by the sensitivity and thermal response time. Sensitivity of WB-bolometer can be enhanced by maximizing ΔT while thermal response time can be minimized by optimizing the thermal isolation legs design.

$$\Delta T_{\max} = \frac{\eta P_{IR}}{G_{th}\left(1+\omega^2+\tau_{th}^2\right)^{1/2}} \tag{3}$$

$$\tau_{th} = C_{th}/G_{th} \tag{4}$$

where G_{th} is the total thermal conductance between the bolometric membrane to its surrounding, C_{th} is the heat capacity of the bolometric membrane, τ_{th} is the thermal time constant, η is the IR absorptivity, P_{IR} is the incident IR power and ω is the IR modulation frequency. From Eq. (3) and (4), G_{th} plays an important role in IR detector performance. The value of G_{th} is determined by the Eq. (5) and (6).

$$G_{th} = G_{leg} + G_{rad} + G_{gas} + G_{conv} \tag{5}$$

$$G_{leg} = n \cdot \left(\frac{\kappa_{leg,1} A_{leh,1}}{l_{leg,1}} + \frac{\kappa_{leg,2} A_{leh,2}}{l_{leg,2}} + \cdots \right) \tag{6}$$

where G_{rad}, G_{leg}, G_{gas} and G_{conv} are the thermal conduction between bolometer and its surrounding through heat radiation, support legs, gas conduction and convection, respectively. Under vacuum environment, G_{gas} and G_{conv} can be ignored and G_{rad} is always negligible compared with G_{leg}. Thus, G_{th} is dominated by G_{leg} which can be designed according to Eq. (6), where n is the number of the bolometer support legs, $\kappa_{leg,x}$, $l_{leg,x}$ and $A_{leg,x}$ are the thermal conductivity, length and cross sectional area of each support leg material, respectively.

G_{th} needs to be small in order to give a high value of ΔT and thus sensitivity. However, decrease in G_{th} results in an increase in τ_{th} as clarified by Eq. (4). Thus, trade-off is needed between sensitivity and speed in the design consideration of the WB-bolometer. In order to increase ΔT while keeping τ_{th} unchanged, one can decrease G_{th} but C_{th} has to be decreased by the same amount as G_{th}. This can be achieved by reducing the bolometric membrane thickness or area. Reducing the bolometric membrane area degrades the sensitivity, thus C_{th} is normally reduced by thinning the bolometric membrane. On the other hand, the support legs should be strong enough to mechanically support the bolometric membrane. Thus, A_{leg} to l_{leg} ratio cannot be too small.

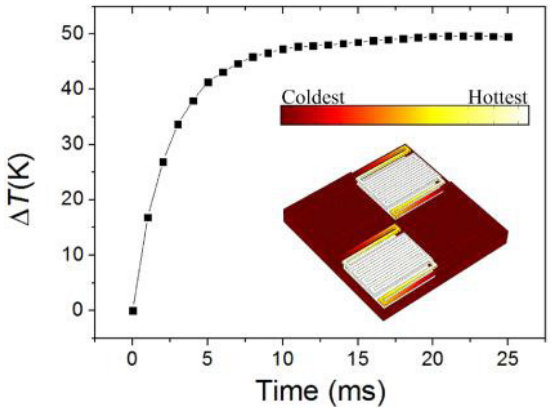

Fig. 5. Simulated temperature profile and thermal response of Design B WB-bolometer at V_s of 0.7 V.

To predict τ_{th} of the Design B WB-bolometer, a time-dependent simulation was carried out using the similar condition settings as those of Section 4.1 by fixing V_s at 0.7 V. The ΔT induced by the Joule heating effect of TiN resistors with time and the temperature profile of Design B WB-bolometer is depicted in Fig 5. It was found that the heat energy from Joule heating of R_s resistors is able to be confined within the SiO_2 freestanding membrane while the temperature of R_f resistors follows the substrate temperature. τ_{th} of the device can be estimated with Eq. 7.

$$T(t) = T(0) + \Delta T\left[1 - \exp\left(-t/\tau_{th}\right)\right] \tag{7}$$

where $T(t)$ is the temperature of R_s at time of t and T (0) is the initial temperature at time zero. The τ_{th} is estimated to be 2.5 ms for Design B WB-bolometer with pixel area of 25 × 25 μm^2, which is superior to the commercial semiconductor-type uncooled microbolometers [17].

4.3. V_o responsivity simulation with IR irradiation heat source

The V_o responsivity with respect to the absorbed IR power, P_{IR} at different levels of P_s for Design B WB-bolometer was studied with the same simulation tool. The condition settings in this simulation are identical with the one in Section 4.1, except that the top surface of TiN was defined with a varying boundary heat source which symbolizes P_{IR}. The simulation results are plotted in Fig 6. A responsivity of about 550 V/W was extracted from the gradient of Fig 6 (b) at the V_s of 0.5 V. Higher V_s gives the higher V_o responsivity at the expense of higher initial offset voltage and noise level. However, this small offset voltage can be easily compensated using software program or readout circuits.

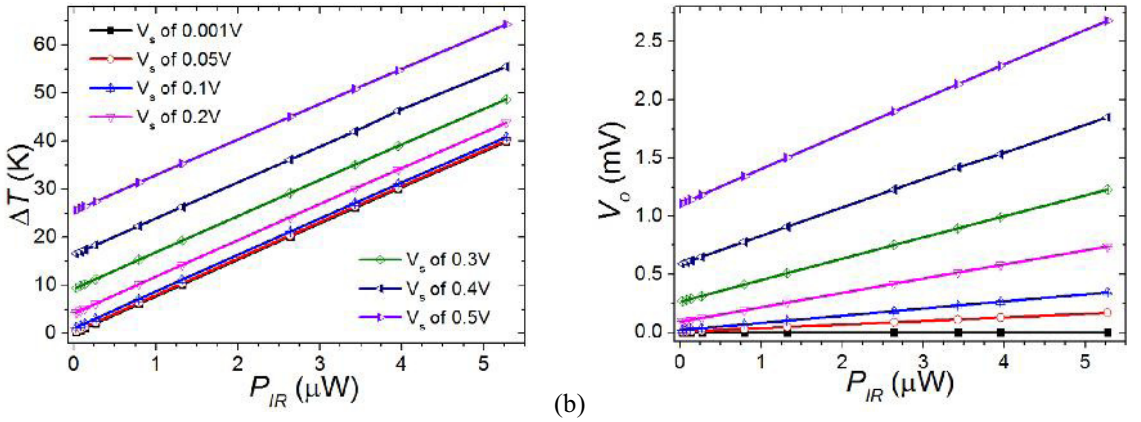

(a) (b)

Fig. 6. (a) Simulated ΔT and (b) V_o of Design B WB-bolometer at increasing V_s and P_{IR}.

5. Conclusion

Three designs of WB-bolometer have been studied through simulation to estimate their performance. It was found that the design with double sensing elements, R_s which located opposite to each other in the Wheatstone bridge, gives the best performance. A responsivity of about 550 V/W is expected from the simulation and this value can be further enhanced with higher voltage supply, V_s at the expense of high initial offset voltage and Johnson noise. Further in depth noise analysis is needed on the fabricated devices in order to determine the

operation conditions for the optimum performance. On the other hand, high temperature operation is possible by using refractory metal like Pt and Au, which have also higher TCR value to compensate the background noise.

Acknowledgements

Authors are grateful to the clean room staffs in Institute of Microelectronics, Singapore for their supports in fabrication process. GLOBALFOUNDARIES Singapore Pte Ltd and Singapore Economic Development Board are acknowledged for the scholarship of the PhD program at Nanyang Technological University. Funding is provided by the Agency for Science, Technology and Research (A*STAR), Singapore (#102165 0084).

References

[1] Breen, T., Butler, N., Kohin, M., Marshall, C. A., Murphy, R., Parker, T., Piscitelli, N., Silva, R., 1999. “A summary of applications of uncooled microbolometer sensors,” Proceeding of the IEEE Aerospace Conference, pp. 361-74.
[2] Rogalski, A., 2003. Infrared detectors: status and trends, Progress in Quantum Electronics 27, p. 59-210.
[3] Rogalski, A., 2011. Recent progress in infrared detector technologies, Infrared Physics & Technology 54, p. 136-54.
[4] Razeghi, M., 1998. Current status and future trends of infrared detectors, Opto-electronics Review 1998, p.155-94.
[5] Hornberger, C., 2002. Application of military uncooled infrared sensors to homeland defense. pp 201-11.
[6] Orvatinia, M., Heydarianasl, M., 2012. A new method for detection of continuous infrared radiation by pyroelectric detectors, Sensors and Actuators A: Physical 174, p. 52-7.
[7] Querner, Y., Schulze, A., Norkus, V., Gerlach, G., 2010. High-sensitive pyroelectric detectors with internal thermal amplification, Procedia Engineering 5, p. 629-32.
[8] Shao, X., Ding, J., Ma, X., Yu, Y., Fang, J., 2012 Design and thermal analysis of electrically calibrated pyroelectric detector, Infrared Physics & Technology 55, p. 45-8.
[9] Dehui, X., Bin, X., Guoqiang, W., Yinglei, M., Yuelin, W., 2012. Uncooled Thermoelectric Infrared Sensor With Advanced Micromachining, IEEE Sensors Journal 12, p. 2014-23.
[10]Hung-Yu, W., Po-Yang, T., Chih-Yi, L., Jyun-Jie, H., 2010. “A CMOS-MEMS Thermoelectric Infrared Sensor,” Proceeding of the International Conference on Electrical and Control Engineering, pp. 19-22.
[11]Kryskowski, D., 2011. “Small pitch high performance thermopile focal plane arrays,” Proceeding of the Infrared Technology and Applications XXXVII, pp. 28.
[12]Bauer, S., Bauer-Gogonea, S., Becker, W., Fettig, R., Ploss, B., Ruppel, W., von Münch, W., 1993. Thin metal films as absorbers for infrared sensors, Sensors and Actuators A: Physical 37, p. 38 497-501.
[13]Gu, X., Karunasiri, G., Chen, G., Sridhar, U., Xu, B., 1998. Determination of thermal parameters of microbolometers using a single electrical measurement, Applied Physics Letters 72, p. 1881-3.
[14]Schoeneberg, U., Hosticka, B.J., Schnatz, F.V., 1990. “A CMOS-Readout-Amplifier For Instrumentation Applications,” Proceeding of the 16th European Solid-State Circuits Conference, pp 133-6.
[15]Narayandass, S.K., Jeyachandran, Y.L., Mangalaraj, D., Areva, S., Mielczarski, J.A., 2007. Properties of titanium nitride films prepared by direct current magnetron sputtering, Materials Science & Engineering A (Structural Materials: Properties, Microstructure and Processing) 445-446, p. 223-36.
[16]Creemer, J.F., van der Vlist, W., de Boer, C.R., Zandbergen, H.W., Sarro, P.M., Briand, D., de Rooij, N.F., 2005. “MEMS hotplates with TiN as a heater material.” Proceeding of the IEEE Sensors, pp. 4.
[17]Kruse, P.W., 1994. “Uncooled infrared focal plane arrays,” Proceedings of the IEEE International Symposium on Applications of Ferroelectrics, pp. 643-6.